

# Improved drill shroud capture of respirable dust utilizing air nozzles underneath the drill deck

W.R. Reed and J.D. Potts

Mining engineers at the Respiratory Hazards Control Branch,  
National Institute for Occupational Safety and Health (NIOSH), Pittsburgh, Pennsylvania

## Abstract

*This study tests the ability of a new air nozzle system, located under the drill deck shroud, to improve the dust capture of the drill deck shroud. The system consists of three air nozzles supplied with regulated pressurized air and located midway down the shroud in the off-inlet corners of the shroud. Laboratory testing produced operating curves for the system that showed an optimum operating point of 207 kPa (30 psi) and generated respirable dust reductions of 48% to 52% from the drill deck shroud.*

## Introduction

Surface mine blasthole drills have been shown to generate large amounts of respirable dust during dry drilling. A past NIOSH study documented that time-weighted average dust concentrations from area sampling in the vicinity of the drill shroud can potentially range from 8.68 to 95.15 mg/m<sup>3</sup> (Organiscak and Page, 1995). Another study corroborated these results, showing area sampling respirable dust concentrations ranging from 1.04 to 52.30 mg/m<sup>3</sup> for dry drilling (Listak and Reed, 2007). These concentrations are highly variable and are dependent on the effectiveness of the dust controls used on the drill, with higher dust concentrations resulting from poor dust control methods.

To put these dust concentrations into perspective, 2.0 mg/m<sup>3</sup> is the maximum allowable respirable dust concentration for exposure at coal mines. If the silica in the respirable dust sample is >5%, then the maximum allowable concentration is reduced to the quotient of 10 divided by the percent silica in the sample. Generally, emissions from drilling operations also contain silica, which continues to be an ongoing concern in the mining industry, as exposure to respirable crystalline silica dust can lead to silicosis. Silicosis is a respiratory disease that is often fatal and has no cure, except through its prevention (Porter and Kaplan, 2007). A review of the Mine Safety and Health Administration (MSHA) database of respirable dust samples containing silica from 2001 to 2004 shows that drilling operators and their helpers have some of the highest exposures to respirable silica dust, with overexposure rates of 19% and 14%, respectively. Additionally, the blaster or shotfirer, who often works near operating surface mine blasthole drills, has an overexposure rate of 9% for respirable silica

dust (Joy, 2005).

Wet drilling is an effective method to reduce dust concentrations, but wet drilling has disadvantages, such as water-freezing issues in northern climates and rotary bit life reductions caused by the use of water during drilling. Therefore, many drilling operations use a dust collector system to control dust emissions. When operating properly, dust collector systems are very efficient. However, as operating parameters change or if the system is poorly maintained, there can be a significant reduction in system efficiency (Listak and Reed, 2007). Therefore, additional dust control methods for dry drilling are being investigated.

Dust from drilling operations generally emanates from three sources on the drill rig: the dust collector dump, the drill stem and the drill shroud (Maksimovic and Page, 1985). The focus of this work was directed toward eliminating dust emissions from the drill shroud. Prior research in this area focused on maximizing dust capture from the drill shroud through the evaluation of collector-to-bailing airflow ratios. This work also showed the importance of minimizing leakage from the drill shroud. Collector-to-bailing airflow ratios of 4:1 (i.e., a collector airflow four times the amount of bailing airflow) were shown to efficiently reduce dust concentrations from the shroud area. However, most drills operate with collector-to-bailing airflow ratios of 2:1 (Page and Organiscak, 2004). Therefore, further investigations were conducted to find additional methods to reduce concentrations. Based on the results of this research, a new method of using air nozzles underneath the drill deck shows promising results for minimizing dust concentrations caused by leakage from the shroud without having to modify



**Figure 1** — Drill deck with shroud showing leakage between the bottom of the shroud and ground surface.

the collector airflow.

### Background of the problem

The drill deck or table, shown in Fig. 1, is located adjacent to the operator's cab, which allows the operator access to perform maintenance on the drilling apparatus. This platform is generally 0.91 m (3 ft) above the ground level. The gap between the bottom of the drill deck and the ground surface, which can range from 0.61 to 1.22 m (2 to 4 ft), is enclosed using conveyor belting or similar material. This enclosure is part of the drill dust collection system, which helps to contain the dust generated during drilling. The dust collector, connected to the drill deck by large diameter wire-reinforced hose, removes dust from under the shroud. The inlet to the dust collection system is generally located on the drill deck at the back corner of the side opposite the operator's cab. Dust leakage from the drill deck enclosure can occur at three different sources. Two of the sources that were evaluated in this study are leakage from gaps between the bottom of the shroud and the ground and from gaps at the corners of the enclosure. The other source of dust is from leakage around the table bushing where the drill steel goes through the drill deck.

During the drilling operation, bailing air is sent through the center of the drill steel, exiting at openings on the drill bit. This bailing air is used to cool the drill bit and to flush the drill cuttings from the hole (Brantly, 1961). The air and the cuttings exit the drill hole at a high velocity. Once the air enters the drill deck enclosure, its velocity is reduced and the large drill cuttings drop out of the air stream. The respirable dust, because of its small size, continues with the airstream, as the reduction of velocity is generally not enough to allow these smaller particles to fall out. The suspended respirable dust leaks from the shroud, resulting in respirable dust emissions. This study evaluated the use of air nozzles for directing dusty air to the scrubber inlet to improve dust capture and reduce the

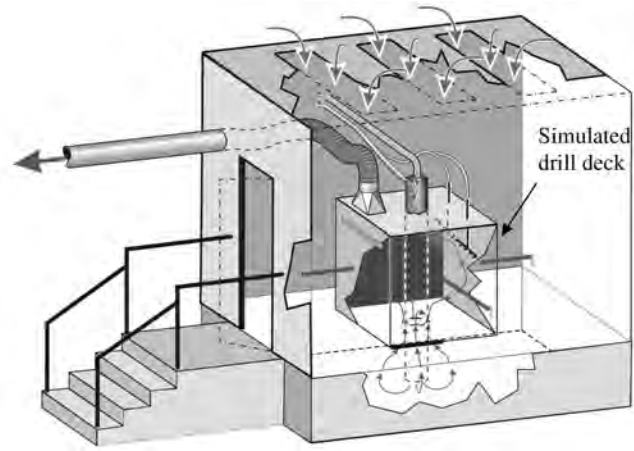


**Figure 2** — Drill deck testing facility at NIOSH.

amount of dust leaking from the shroud. Different air nozzle configurations underneath the shroud were tested on a drill shroud simulator that was constructed at NIOSH labs.

### Test facility

NIOSH's test facility used for the air nozzle testing has been thoroughly described in previous publications (Page and Organiscak, 2004; Organiscak and Page, 2005). This facility, which simulates the dust collection system of a blasthole drill rig, is used to evaluate dust control techniques for surface drills in a controlled laboratory environment. The laboratory environment includes a full-scale model of a drill deck and shroud as shown in Fig. 2.

The simulator is contained in a large dust chamber, which serves as a containment and monitoring area for the dust that escapes the shroud. To prevent dust from leaking outside of the chamber, static pressure in the chamber is controlled and maintained by a series of louvered vents located on the top of the chamber. The simulated drill deck and shroud, whose dimensions are 1.52 m wide, 1.22 m deep and 1.22 m high (5 by 4 by 4 ft), are located in the center of the dust chamber. This shroud size is within the range found on medium-sized rock drills (rubber-tired or track-mounted) that drill holes 127 to 203 mm (5 to 8 in.) in diameter, with about 178 to 222 kN (40,000 to 50,000 lbs) of drill pulldown pressure. The base of the shroud is fitted with hinged plywood slats that can be adjusted to simulate gaps between the ground and the shroud, from which dust escapes. The gaps can be set at a range of 51 to 356 mm (2 to 14 in.).

Compressed air, using a Kaiser DSD125 air compressor capable of delivering 326 L/s at 758 kPa (690 cfm at 110 psi), is piped into the simulated drill steel to represent the bailing air of the drill rig during the drilling process. A 152-mm (6-in.) steel pipe, which extends from 0.61 m (2 ft) above the simulated drill deck to 0.91 m (3 ft) beneath the floor of the test chamber, is used to simulate the drill steel. This 152-mm (6-in.) pipe is concentrically located in a 203-mm (8-in.) steel pipe. This 203-mm (8-in.) pipe simulates the drill hole with its opening at the chamber floor surface; it extends from the floor to 0.91 m (3 ft) beneath the floor of the chamber. The pressure and flow rate can be regulated to provide accurate bailing air velocities. To simulate the dust emissions from the borehole, a Vibra-Screw feeder delivers the amount of limestone rock dust (approximately 25 g/min) at a constant rate into a compressed air

eductor, operating on a small separate split of air at 11.8 L/s (25 cfm). The limestone dust has a particle size distribution similar to the bulk dust at the dust collector dump point. Figure 3 shows the mass frequency of the particle size of the test material with the bulk dust collector material and illustrates the similarities in particle size distributions. This dust is mixed with the remaining bailing airflow near the top of the 152-mm (6-in.) pipe and blown out the concentric opening between the 152-mm (6-in.) pipe and the 203-mm (8-in.) pipe. The respirable dust concentrations escaping the shrouded area over this simulated drill hole is the response variable measured during these experiments, while maintaining a constant feed rate with the Vibra-Screw feeder.

As with a rotary drill rig, the simulator's dust collector provides the negative pressure within the shroud to collect the dust as it is emitted from the hole at the base of the chamber. The dust collector was simulated using a baghouse connected through fiberglass tubing. The final connection to the drill deck was accomplished using 203-mm- (8-in.-) diameter wire-reinforced tubing, which connected using a metal transition from 203-mm- (8-in.-) diameter to a 457- by 190.5-mm (18- by 7.5-in.) rectangular opening in the drill deck. The collector is capable of providing variable flow rates up to a maximum flow of 944 L/s (2,000 cfm). The collector's inlet is located in the corner of the simulator, similar to those found on drills in the field.

### Preliminary testing

Preliminary experiments were conducted to determine the viability and the optimum placement of the air nozzles for maximized dust capture of the drill shroud and to narrow these variable ranges for a factorial design experiment. Variables investigated included spray location, orientation, quantity, type and pressure. The air nozzles evaluated were flat-fan and hollow-cone plastic air nozzles (Spraying Systems Co. WindJet Models AA727-11 and AA707-11, respectively). These nozzles were chosen because they do not require large quantities of air from the compressor and thus are able to generate airflow without affecting the bailing airflow quantity.

Dust measurements were made with two RAM sampling devices located outside of the shroud on the front (on-inlet) and back (off-inlet) sides. The locations are shown in Fig. 4 and are labeled as RAM-Front and RAM-Back. The locations of the gravimetric sampling, which was not conducted during the preliminary testing, are also shown and are numbered consecutively from 1 to 8. The RAM data were fed into a chart recorder and a data recorder to provide an instantaneous visual representation of dust concentrations and to allow downloading of data for post-test analysis. The preliminary tests followed an ABAB pattern, where A was the spray-off condition and B was the spray-on condition, with each segment lasting 10 minutes.

Initially, horizontal spray bars containing four in-line nozzles were tested at various locations underneath the shroud, as shown in Fig. 5 (a). The variables considered in this evaluation were one and two spray bars (four or eight nozzles, respectively), hollow-cone and flat-fan nozzles and air pressures ranging from 34 to 276 kPa (5 to 40 psi). None of the locations tested produced consistent significant reductions of respirable dust outside of the shroud. An attempt was made to push all the airflow from the off-inlet side towards the collector by using

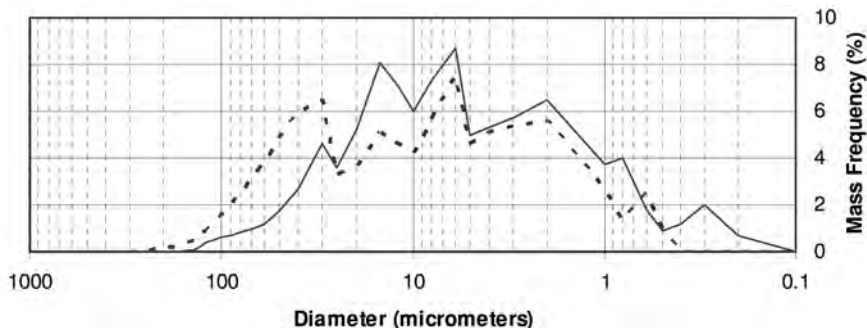


**Figure 3** — Mass frequency of particle diameters of limestone test material (dashed line) compared with bulk dust collector material (solid line).

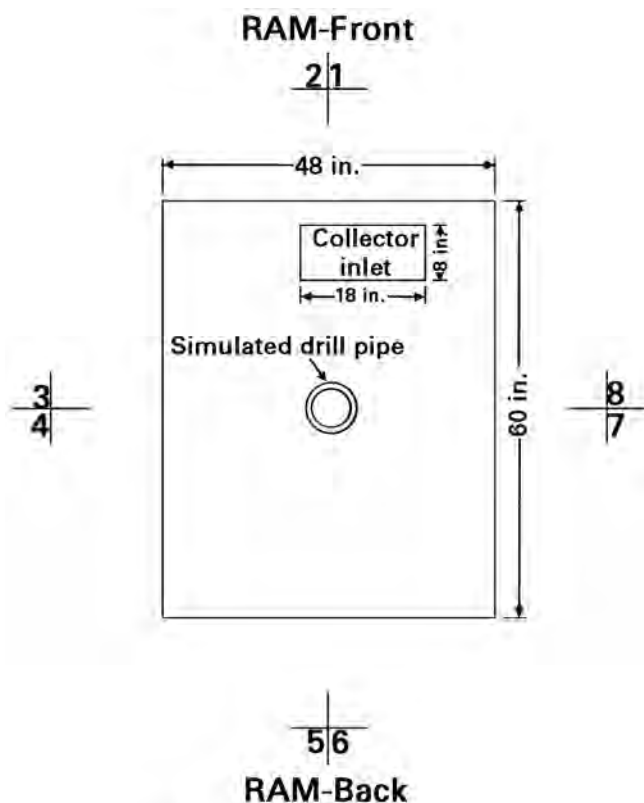


**Figure 4** — Plan view of shroud inside the drill deck testing facility showing the locations of the gravimetric sampling locations (numbered locations) and instantaneous sampling locations (RAM-Front and RAM-Back).

20 air nozzles in a grid pattern on the off-inlet wall, which is opposite the collector inlet, shown in Fig. 5 (b). This evaluation utilized hollow-cone sprays with air pressures ranging from 138 to 552 kPa (20 to 80 psi). This configuration also resulted in unsatisfactory results, sometimes producing more respirable dust emissions, especially at higher pressures. Another configuration placed a set of four hollow-cone nozzles directed into the collector inlet, shown in Fig. 5 (c), at pressures ranging from 34 to 276 kPa (5 to 40 psi). These operating pressures produced dust reductions at the 69 and 138 kPa (10 and 20 psi) levels. However, these reductions were inconsistent and varied from 3.0% to 26.0%, with the best reductions



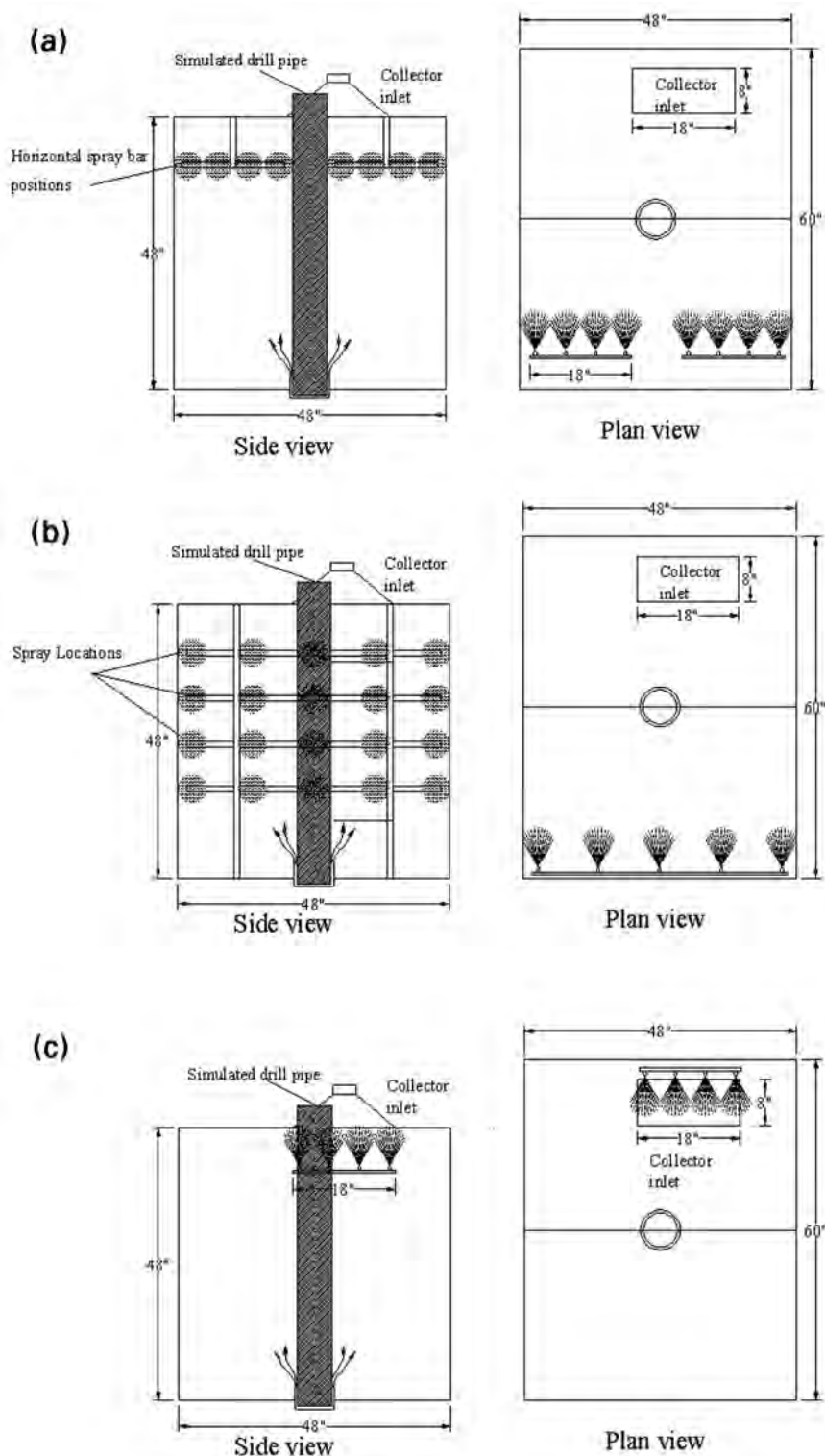


**Figure 5** — Spray locations that were ineffective in reducing respirable dust concentrations: (a) horizontal spray bar positions, (b) 20 pushing spray locations and (c) inlet spray locations.

occurring at 138 kPa (20 psi). Due to the inconsistency of the reductions, it was decided that these three test scenarios were not worth evaluating.

The nozzle orientation evaluated during preliminary testing that showed the most potential for respirable dust reductions

was a vortex configuration with the nozzles placed midway down the shroud and oriented slightly off parallel (a slight angle of  $<10^\circ$ ) from the side of the shroud. The vortex configuration targeted airflow in a clockwise direction underneath the shroud, in a manner similar to the rotation of the drill steel. Initial testing involved as many as 20 sprays with pressures ranging from 69 to 276 kPa (10 to 40 psi); however, dust reductions were not observed until the number of sprays was decreased to four. Throughout preliminary testing of the vortex orientation, three sprays produced as good or better results than four sprays. Two sprays demonstrated a marked drop in performance. Therefore, in the interest of minimizing air consumption but maintaining system integrity, the factorial experiment only examined a three-spray system. Figure 6 shows the placement of the three effective air nozzles.

The impacts of spray pressure and nozzle type (flat-fan vs. hollow-cone) on dust levels were not as easily discernable during preliminary testing. These variables were included in the factorial experiment for further analysis. During the preliminary test, this three-spray configuration produced a stark contrast between the on and off conditions, reducing average dust levels at the front and back sides of the shroud by 67% and 54%, respectively. Using results from the preliminary testing, the following factorial experiment design was formulated to further investigate the use of air as a means of improving dust capture under the shroud.

### Test procedure

The drill deck simulator was used for testing the vortex air nozzle configuration. The shroud-to-ground gap was kept at a constant 51 mm (2 in.) throughout testing. Higher gap settings were not used because drill operators are generally conscientious about minimizing leakage between the ground and the bottom of the shroud. Bailing air was supplied to the facility in two separate splits. The main split of air was regulated between 226 and 234 L/s (479 and 495 cfm) averaging 230 L/s (488 cfm) after temperature and pressure correction for the deviations from the conditions at which the flow meter was calibrated. The main split temperature varied from 17° to 26°C (62° to 78°F) and the pressure for all tests was 207 kPa (30 psi). The secondary split of air for the dust feed was regulated at 11.8 L/s (25 cfm) after temperature and pressure correction. The secondary split temperature varied from 18° to 28°C (65° to 82°F) and the pressure was maintained at 345 kPa (50 psi). Therefore, the total bailing airflow rate varied between 237 and 246 L/s (503 and 521 cfm).

To provide the dust feed, the secondary air split was used

to drive a venturi eductor. The eductor and secondary air split injected test dust into the main split of air at the head of the simulated drill pipe location. Limestone sized to 100% <math><0.25\text{ mm}</math> (60 mesh) was used as a test dust and fed into the eductor by a Vibra-Screw feeder equipped with a 13-mm- (0.5-in.-) diameter auger feed screw. The feed rate ranged from 23.1 to 27.4 g/min, targeting a sustainable feed rate to be maintained within  $\pm 10\%$  of the average of 25.1 g/min. This feed rate was selected over the lower feed rates previously used (Organiscak and Page, 2005) in an attempt to simulate the high dust concentrations encountered during previous area sampling of drilling operations (Organiscak and Page, 2005; Listak and Reed, 2007).

A dust-collector-to-bailing-airflow ratio of 2:1 was targeted throughout the testing. Dust collector airflows ranged from 447 to 480 L/s (947 to 1,018 cfm) with an average of 462 L/s (978 cfm). These airflows were calculated from velocity pressures measured before and after each test. Measurements were performed using a pitot tube inserted into the fiberglass tubing dust collector network. The resulting dust collector airflows produced collector-to-bailing airflow ratios ranging from 1.87 to 2.00, with an average ratio of 1.91. This dust-collector-to-bailing-air ratio is representative of the typical operation of a dust collector on a rotary blasthole drill (Page and Organiscak, 2004).

Gravimetric samplers using 37-mm filter cassettes and 10-mm Dorr-Oliver cyclones were used to measure respirable dust levels inside the chamber. Two samplers were used on each of the four sides of the shroud and located approximately 0.61 m (2 ft) above the floor level, yielding a total of eight gravimetric samples for each test. Figure 4 shows the gravimetric sampler locations, which are numbered consecutively from 1 to 8, and the instantaneous RAM sampler locations labeled RAM-Front and RAM-Back. All gravimetric samplers maintained constant flow rates of 2.0 L/min using one vacuum pump. Consequently, all samplers were turned on/off simultaneously. All of the gravimetric sampler flow rates were calibrated prior to conducting the series of tests. Two RAM-1 instantaneous dust monitors were used at the on-inlet and off-inlet sides of the drill deck with the RAM sampler head located in the same proximity as the gravimetric samplers. The RAM monitors were used to monitor the dust concentration prior to test initiation, during which the pre-test dust feed was adjusted to the proper levels and maintained throughout the test. The analog output of the RAM monitors were fed to a strip chart recorder for visual monitoring of the dust concentration stability and to a data-logging device to allow downloading of the data for later analysis. Dust sampling time was fixed at 30 min after verification that the chamber dust concentration had stabilized. The final chamber dust concentration was determined from the average of the eight gravimetric samples.

Testing examined the effects of the following three variables: nozzle type (flat-fan or hollow-cone); pressure at 138, 207 and 276 kPa (20, 30 and 40 psi); and vertical leakage, which represents possible gaps at the corners of the shroud (no leakage vs. vertical leakage). In other words, this procedure evaluated twelve configurations of nozzle type, pressure, and vertical leakage (2 x 3 x 2). Each configuration, including the

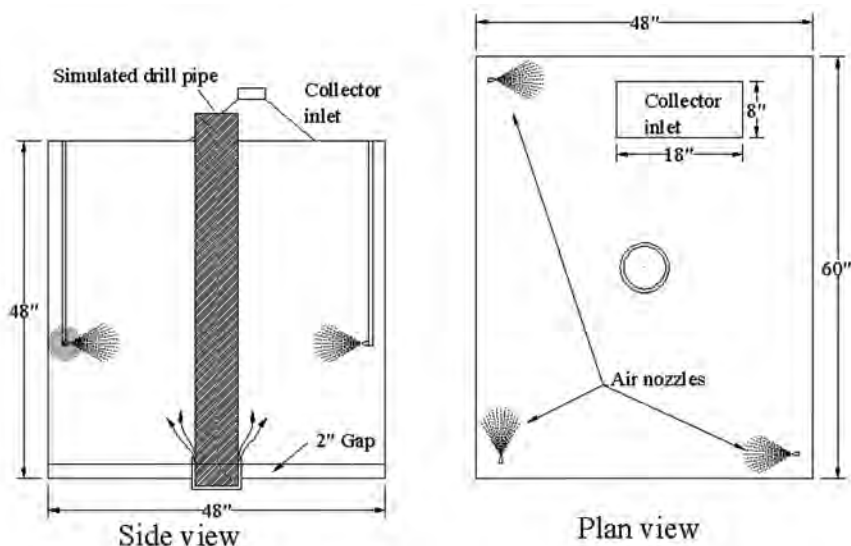


**Figure 6** — Air nozzle spray system using the vortex configuration that is effective at reducing respirable dust concentrations from the drill deck shroud.

baseline where no nozzles were used, was evaluated three times. This resulted in a total of 42 tests, which were conducted in random order. During testing, ambient air data, which included wet and dry bulb temperatures and barometric pressure, were measured outside the test chamber and recorded.

The 138, 207 and 276 kPa (20, 30 and 40 psi) pressures were selected as showing potential for respirable dust reduction during preliminary testing. Lower pressures below 138 kPa (20 psi) only produced slight dust reductions and therefore were not tested. Higher pressures tended to generate too much airflow under the shroud, which increased respirable dust emissions. Vertical leakage was examined to determine its effect on air nozzle operation, as many shrouds are constructed using one piece of conveyor belting per side, due to ease of installation and to allow for expansion as the drill cutting pile becomes larger. Where the pieces of conveyor belting meet at each corner, there is a split through which respirable dust emissions may escape. The vertical leakage was replicated by cutting two 25-by-800 mm (1-by-31.5 in.) slots in the off-inlet side of the drill deck simulator, each at a location nearest the corner. The slots were covered when vertical leakage was not desired during testing.

## Results

Table 1 shows the gravimetric and instantaneous respirable dust concentrations for each configuration, sorted by spray type, spray pressure and vertical leakage. The figures reported for the back and front gravimetric concentrations are averaged from the samples taken at locations 5 and 6 (back) and 1 and 2 (front), respectively (see Fig. 4). The average gravimetric concentration is calculated from samples taken at all eight locations (individual sample results are not shown). In contrast, the back and front instantaneous concentrations are the average of all back (RAM-back) and front (RAM-front) instantaneous concentrations, respectively, that were recorded at 10-second intervals for the entire 30-minute testing period, with the average instantaneous concentration being the average of the back and front instantaneous concentrations.

Figures 7 and 8 show the graphs of the gravimetric respirable dust concentrations versus air nozzle pressure for both

**Table 1** — Respirable dust concentrations from air nozzle testing.

Test	Spray type	Spray pressure, psi	Vertical leakage	Gravimetric concentrations			Instantaneous concentrations		
				Back, mg/m <sup>3</sup>	Front, mg/m <sup>3</sup>	Average, mg/m <sup>3</sup>	Back, mg/m <sup>3</sup>	Front, mg/m <sup>3</sup>	Average, mg/m <sup>3</sup>
32	FF	20.0	no	4.80	10.24	7.43	4.22	8.65	6.44
35	FF	20.0	no	4.53	11.47	7.60	4.00	9.16	6.58
20	FF	20.0	no	8.06	12.66	10.53	7.45	10.20	8.82
41	EF	30.0	no	4.07	4.67	5.32	3.57	4.04	3.81
15	FF	30.0	no	7.38	7.11	7.84	6.64	5.74	6.19
3	FF	30.0	no	7.98	6.96	8.13	7.08	5.99	6.53
24	FF	40.0	no	7.94	8.54	8.14	7.47	6.98	7.23
34	FF	40.0	no	7.75	8.35	8.31	7.32	6.96	7.14
31	FF	40.0	no	8.07	8.68	8.74	6.55	7.44	6.99
23	FF	20.0	yes	12.50	9.23	11.35	10.69	7.49	9.09
28	FF	20.0	yes	14.14	10.96	13.06	12.39	8.88	10.64
4	FF	20.0	yes	14.01	10.70	13.20	12.24	8.76	10.50
14	FF	30.0	yes	11.17	7.75	10.01	9.87	6.32	8.10
17	FF	30.0	yes	10.86	7.99	10.23	9.91	6.25	8.08
8	FF	30.0	yes	14.52	7.88	11.73	12.21	6.40	9.30
1	FF	40.0	yes	11.27	9.20	11.92	11.65	7.56	9.60
27	FF	40.0	yes	13.79	11.14	11.98	12.05	8.97	10.51
33	FF	40.0	yes	18.33	14.73	15.65	15.88	11.90	13.89
11	HC	20.0	no	7.19	5.50	7.49	6.96	4.49	5.73
10	HC	20.0	no	7.70	6.43	8.15	6.53	5.35	5.94
19	HC	20.0	no	6.13	12.12	8.72	5.49	9.55	7.52
42	HC	30.0	no	4.12	4.60	5.44	3.44	4.38	3.91
38	HC	30.0	no	5.16	8.44	6.95	4.54	6.83	5.68
39	HC	30.0	no	5.38	8.04	7.34	4.35	7.13	5.74
36	HC	40.0	no	6.29	6.45	6.78	5.32	5.07	5.20
21	HC	40.0	no	6.85	6.63	7.48	5.86	5.66	5.76
6	HC	40.0	no	8.32	7.53	8.07	6.97	6.09	6.53
5	HC	20.0	yes	11.61	7.31	9.42	8.71	6.16	7.43
12	HC	20.0	yes	11.23	7.36	9.57	10.57	5.86	8.22
13	HC	20.0	yes	12.70	9.35	11.17	11.48	7.78	9.63
13b	HC	20.0	yes	14.13	12.27	13.14	12.77	9.82	11.29
16	HC	30.0	yes	12.92	10.38	12.49	11.51	8.21	9.86
29	HC	30.0	yes	15.97	9.84	13.24	14.27	8.41	11.34
30	HC	30.0	yes	17.01	11.23	14.51	13.96	9.57	11.77
37	HC	40.0	yes	12.47	9.77	10.48	11.65	8.02	9.84
25	HC	40.0	yes	13.31	9.08	11.75	10.55	7.33	8.94
9	HC	40.0	yes	14.08	8.63	12.32	11.89	7.13	9.51
2	none	-	no	12.72	9.61	11.78	12.66	8.14	10.40
22	none	-	no	10.86	12.50	12.70	9.97	10.42	10.19
7	none	-	no	15.38	14.31	16.38	14.38	12.01	13.20
40	none	-	yes	10.60	9.80	11.45	8.45	8.50	8.48
18	none	-	yes	10.38	10.02	11.91	8.70	8.50	8.60
26	none	-	yes	11.82	10.76	13.37	9.31	8.94	9.13

Note: Average gravimetric concentration includes gravimetric concentrations from four drill deck samples, which are not shown.  
FF = Flat-Fan  
HC = Hollow-Cone

the flat-fan and hollow-cone spray nozzles, respectively. These graphs were created by averaging the time-weighted average gravimetric dust concentration results of the three tests of each case that was evaluated during this study and plotting these results with their corresponding pressure.

The results in Fig. 7 show the operating performance curve that was fit to the gravimetric dust concentration data for flat-

fan nozzles. This curve uses a second-order polynomial to fit the data and had an R-squared value of 98.7%, demonstrating a good fit to the data. Use of the flat-fan air nozzles resulted in a dust concentration reduction outside the shroud of approximately 48% when the nozzles were operated at 207 kPa (30 psi). Operating the nozzles at lower or higher operating pressures, i.e., 138 and 276 kPa (20 and 40 psi), resulted in less dust



reduction (37% and 38%, respectively). However, whenever vertical leakage was present in the shroud, the operation of the air nozzles did not appear to influence the dust concentrations.

Figure 8 shows the operating performance curve for the hollow-cone nozzles. This curve also used a second-order polynomial to fit the data and had an R-squared value of 99.3%, demonstrating a good fit to the data. Use of the air nozzles resulted in a dust concentration reduction outside the shroud of approximately 52% when the nozzles were operated at 207 kPa (30 psi). Operating the nozzles at lower or higher operating pressures, i.e., 138 and 276 kPa (20 and 40 psi), resulted in less dust reduction (40% and 45%, respectively). Again, however, vertical leakage appeared to negate the benefit of using air nozzles for reducing dust.

Figure 9 shows the graph of the instantaneous respirable dust concentrations versus air nozzle pressure for both the flat-fan and hollow-cone spray nozzles without vertical leakage. This graph was created by averaging all the instantaneous respirable dust concentrations for the 30-minute testing period of the three tests for each case evaluated, then plotting these results with their corresponding pressure. Figure 9 supports the gravimetric results shown in Figs. 7 and 8, producing dust concentrations outside the shroud that are 51% lower when operating flat-fan nozzles at 207 kPa (30 psi) and 55% lower when operating hollow-cone nozzles at 207 kPa (30 psi). Again, it is demonstrated that operating the nozzles at lower or higher pressures, i.e., 138 and 276 kPa (20 and 40 psi), results in less dust reduction (35% and 37%, respectively, for flat-fan nozzles and 43% and 48%, respectively, for hollow-cone nozzles) than operating at 207 kPa (30 psi).

## Discussion

At the start of the design process, it was thought to be important to orient the nozzles to target the airflow in a clockwise direction, similar to the drill steel rotation. The reasoning was that the nozzles produced a vortex underneath the shroud that would help move the dust from the off-inlet sides of the drill deck shroud towards the collector inlet. However, further investigation of the airflow underneath the drill deck revealed that this was not the case. A qualitative airflow model was developed using smoke tubes and a tuft grid technique (SAE, 1986), which uses a mesh and streamers to visualize the flow directions. One side of the shroud was constructed of transparent acrylic plastic to allow observation of the area enclosed by the shroud. The tuft grid was created by

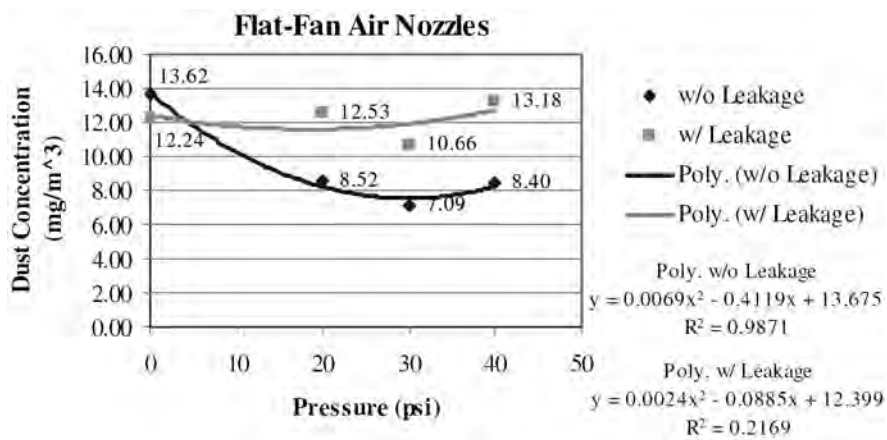


Figure 7 — Respirable dust reduction curves for flat-fan air nozzles, both with and without vertical leakage, using time-weighted average gravimetric data.

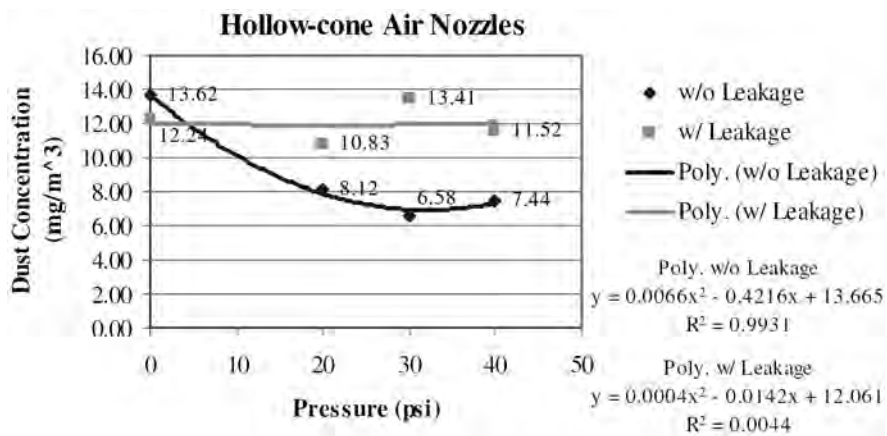


Figure 8 — Respirable dust reduction curves for hollow-cone air nozzles, both with and without vertical leakage, using time-weighted average gravimetric data.

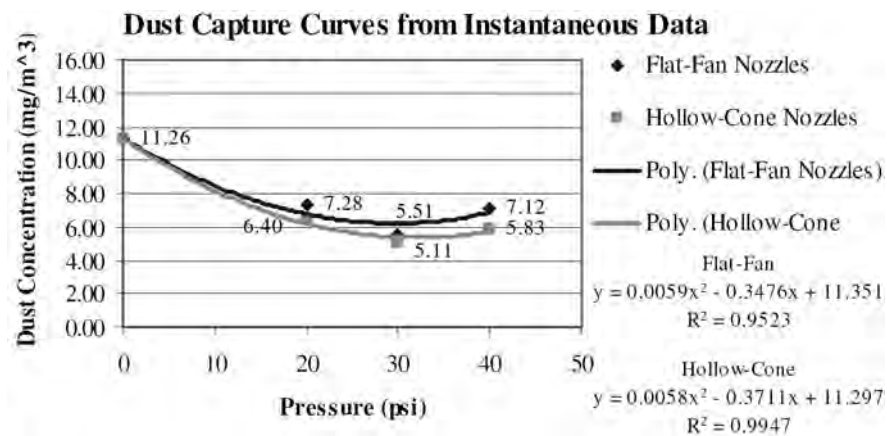
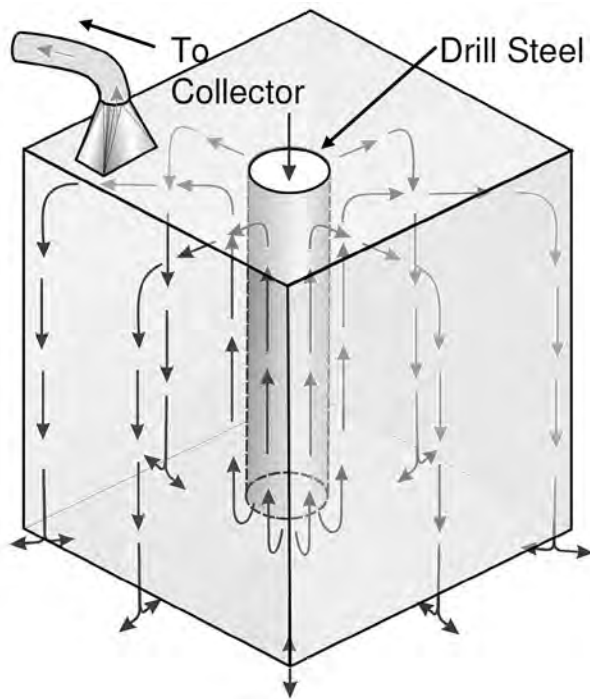


Figure 9 — Respirable dust reduction curves for flat-fan and hollow-cone air nozzles without vertical leakage using instantaneous dust concentration data.



**Figure 10** — Airflow patterns underneath the drill shroud (arrows represent airflow).

attaching lightweight vinyl streamers to a wire mesh, which was cut to the same dimensions as the horizontal parametric cross-section of the shroud enclosure. Airflow patterns were observed at various heights under the shroud during operation of the drill simulator to develop the qualitative model shown in Fig. 10. The arrows in Fig. 10 represent the bailing airflow, with the large downward arrow at the top center of the drill shroud representing the bailing airflow through the drill steel and other arrows depicting the airflow after the bailing air leaves the drill hole.

The airflow underneath the drill shroud, from the drill hole, was discovered to follow along the drill steel up to the bottom of the drill table. Once the air hits the underside of the drill table, the airflow radiates 360° from the drill steel and follows the bottom side of the drill table. Once the airflow hits the shroud at the edge of the drill table, it flows down the shroud on all sides, hitting the ground surface. Smoke tubes demonstrated that a portion of the air hitting the ground dispersed outside of the shroud, resulting in dust leakage into the environment. The space underneath the shroud between the air flowing up along the drill steel and the air flowing down the side of the shroud is predominantly dead air space, with airflow drifting toward the collector inlet. In evaluating the placement of the nozzles and the airflow underneath the drill deck, it is more likely that the air stream from the nozzle disrupts the airflow coming down the shroud and redirects it into the dead air space, thereby causing the reduction of dust concentrations emanating from the bottom of the shroud.

The operating curves for the air nozzle system shown in Figs. 7 and 8 use a second-order polynomial to fit the data. This provides the best fit as shown by the R squared values (98.7% flat-fan, 99.3% hollow-cone). A linear curve would not provide a good fit to the data as seen by the rise in dust

concentrations at the higher operating pressure of 276 kPa (40 psi). Examining Figs. 7, 8 and 9 shows that the optimum operating point for dust reduction is at 207 kPa (30 psi). Beyond the 207 kPa (30 psi) operating point, the dust concentrations begin to rise. The increasing pressure causes an increase in airflow from the nozzles underneath the shroud. This extra airflow into the shroud area can result in a lowering of the collector-to-bailing airflow ratio (i.e., < 2:1 from the lab experiments), which can lead to a reduction of the efficiency of the dust collection system (Page and Organiscak, 2004). The additional airflow also reduces the amount of negative pressure in the system, creating a condition of positive pressure, which results in higher levels of leakage and dust. Testing was not performed to determine whether this optimal operating point was universal for other configurations and dimensions of the drill deck shroud component of the dust collection system. Therefore, these performance curves for the air nozzle system may only be applicable to drill deck shrouds that are similar in configuration and dimensions of the shroud in this test facility.

Figure 9 depicts both operating curves for the flat-fan and the hollow-cone nozzles using the instantaneous data recorded during testing. These curves corroborate 207 kPa (30 psi) as an optimal operating pressure for the air nozzle system. However, they additionally show that the type of spray is not very important in the operation of the system. The curves from the gravimetric dust concentration data also support this view. Hollow-cone nozzles are shown to be slightly more efficient at dust reduction than the flat-fan nozzles, but this advantage is not significant when looking at the dust reductions of 48% and 52% for flat-fans and hollow-cones, respectively. It would be preferable to use hollow-cones, but the placement of the nozzles in the corners and maintaining their parallel orientation with the side of the drill shroud is more important.

## Conclusion

A new air nozzle system was devised to help improve dust capture from underneath the drill deck shroud. This system would be installed underneath the drill deck shroud and consists of three nozzles located midway down the shroud with each nozzle located in the off-inlet corners of the deck as shown in Fig. 6. They would be oriented to provide airflow slightly off-parallel to the side of the shroud (a slight angle <10° away from the shroud). Each nozzle is supplied with regulated pressurized air from the drill's air compressor.

The advantage to this system is that it has been shown to greatly reduce respirable dust concentrations from the drill deck shroud. For the drill deck shroud configuration tested, i.e., 1.52 m wide, 1.22 m deep and 1.22 m high (5 x 4 x 4 ft), operating the air nozzles at 207 kPa (30 psi) reduced dust concentrations by 48% and 52% for flat-fan and hollow-cone nozzles, respectively. It was important during the operation of this system to minimize any vertical leakage, as the presence of vertical leakage negated the benefits of this air nozzle system. Operating the nozzles at lower or higher pressures did not generate dust reductions as great as the optimum operating point of 207 kPa (30 psi). Further testing would be required to determine the optimum operating point of the system if the drill deck shroud configuration were to be changed.

Disadvantages for the use of this system are that it requires the nozzles to be plumbed into the existing compressed air system. This requires additional air lines and regulators to operate and control the system. However, the airflow requirements of the nozzles should not encumber the compressor system, as the three air nozzles use less than 14.2 L/s (30 cfm) of air, com-



bined, at the 207 kPa (30 psi) operating point. Additionally, the nozzles are located underneath the drill shroud. Therefore, they are susceptible to damage when the drill operates in locations where the ground surface undulates greatly. Also, this location underneath the drill shroud makes it difficult for the operator to know when damage has occurred, which could render the system ineffective. Because of these disadvantages, this system would require additional attention in the form of inspections and maintenance to ensure proper operating condition.

Laboratory testing suggests that use of this air nozzle spray system would significantly reduce mine dust exposures from surface mine blasthole drilling operations. This research has investigated the airflow conditions underneath the drill deck shroud when drilling occurs. From these investigations, an air nozzle system has been proposed which can reduce respirable dust concentrations by 48% to 52%. The next step should be to conduct additional field studies on surface mine blasthole drills to validate these reductions as seen in the laboratory. In an effort to reach a goal that mine dust exposures can be fully eliminated from drilling operations, research continues to explore additional innovative methods to eliminate dust exposure from the drill deck shroud, including field trials on surface mine blasthole drills.

## References

- Brantly, J.E., 1961, *Rotary Drilling Handbook*, 6th Edition, Palmer Publications, Los Angeles, California.
- Joy, G.J., 2005, Personal contact about surveillance analysis of MSHA's dust sampling database housed at the US Department of Labor, Mine Safety and Health Administration, Program Evaluation and Information Resources, MSHA Standardized Information System, Arlington, VA.
- Listak, J.M., and Reed, W.R., 2007, "Water separator shows potential for reducing respirable dust generated on small-diameter rotary blasthole drills," *International Journal of Mining, Reclamation, and Environment*, Vol. 21, No. 3.
- Maksimovic, S.D., and Page, S.J., 1985, *Quartz Dust Sources During Overburden Drilling at Surface Coal Mines*, United States Bureau of Mines Information Circular 9056.
- Organiscak, J.A., and Page, S.J., 1995, *Assessment of Airborne Dust Generated from Small Truck-Mounted Rock Drills*, United States Bureau of Mines Report of Investigations 9616.
- Organiscak, J.A., and Page, S.J., 2005, "Development of a dust collector inlet hood for enhanced surface mine drill dust capture," *International Journal of Surface Mining, Reclamation, and Environment*, Vol. 19, No. 1, March, pp. 12-28.
- Page, S.J., and Organiscak, J.A., 2004, "Semi-empirical model for predicting surface coal mine drill respirable dust emissions," *International Journal of Surface Mining, Reclamation, and Environment*, Vol. 18, No. 1, pp. 42-59.
- Porter, R.S., and Kaplan, J.L., eds., 2007, *The Merck Manual of Diagnosis and Therapy*, Online Edition, accessed at [www.merck.com/mmpe/index.html](http://www.merck.com/mmpe/index.html), Merck Research Laboratories.
- Society of Automotive Engineers (SAE), 1986, "Aerodynamic Flow Visualization Techniques and Procedures," *SAE Information Report HS J1566 JAN86*, Society of Automotive Engineers, Inc., Warrendale, Pennsylvania.